Journal of Computational Mathematics
Vol.39, No.4, 2021, 518–537.

http://www.global-sci.org/jcm
doi:10.4208/jcm.2002-m2019-0305

SUB-OPTIMAL CONVERGENCE OF DISCONTINUOUS GALERKIN METHODS WITH CENTRAL FLUXES FOR LINEAR HYPERBOLIC EQUATIONS WITH EVEN DEGREE POLYNOMIAL APPROXIMATIONS*

Yong Liu
School of Mathematical Sciences, University of Science and Technology of China, Hefei 230026, China
Email: yong123@mail.ustc.edu.cn
Chi-Wang Shu[1)]
Division of Applied Mathematics, Brown University, Providence, RI 02912, USA
Email: chi-wang_shu@brown.edu
Mengping Zhang
School of Mathematical Sciences, University of Science and Technology of China, Hefei 230026, China
Email: mpzhang@ustc.edu.cn

Abstract

In this paper, we theoretically and numerically verify that the discontinuous Galerkin (DG) methods with central fluxes for linear hyperbolic equations on non-uniform meshes have sub-optimal convergence properties when measured in the L^2-norm for even degree polynomial approximations. On uniform meshes, the optimal error estimates are provided for arbitrary number of cells in one and multi-dimensions, improving previous results. The theoretical findings are found to be sharp and consistent with numerical results.

Mathematics subject classification: 65M60, 65M15
Key words: Discontinuous Galerkin method, Central flux, Sub-optimal convergence rates

1. Introduction

A fundamental form of energy transmission is wave propagation, which arises in many fields of science, engineering and industry, such as petroleum engineering, geoscience, telecommunication, and the defense industry (see [8, 12]). It is important for these applications to study efficient and accurate numerical methods to solve wave propagation problems. Experience reveals that energy-conserving numerical methods, which conserve the discrete approximation of energy, are favorable, because they are able to maintain the phase and shape of the waves more accurately, especially for long-time simulation.

Various numerical approximations of wave problems modeled by linear hyperbolic systems can be found in the literature. Here, we will focus on the classical Runge-Kutta DG method of Cockburn and Shu [6]. There are several approaches to obtain an optimal, energy conserving DG method. Chung and Engquist [4] presented an optimal, energy conserving DG method for the acoustic wave equation on staggered grids. Chou et al. [3] proposed an optimal energy conserving DG using alternating fluxes for the second order wave equation. More recently, Fu

* Received December 21, 2019 / Revised version received February 19, 2020 / Accepted February 26, 2020 / Published online May 25, 2021 /
1) Corresponding author

and Shu [9] developed an optimal energy conserving DG method by introducing an auxiliary zero function.

As is well known, the simplest energy conserving DG method for hyperbolic equations is the one using central fluxes. However, it has sub-optimal convergence of order k measured in the L^2-norm when piece-wise polynomials of an *odd* degree k are used; see, e.g. [15]. When k is even, we usually observe higher convergence rates than kth order for a general regular non-uniform meshes, such as random perturbation over an uniform mesh, see section 4. In fact, many papers have mentioned that the optimal convergence rates can be observed when even degree polynomials are used; see for example [1, 2, 7, 15]. In this paper, we provide a counter example to show that the scheme only has sub-optimal error accuracy of order k for a regular non-uniform mesh, when k is even. We refer to the work of Guzmán and Rivière [11] in which they constructed a special mesh sequence to produce the sup-optimal accuracy for the non-symmetric DG methods for elliptic problems when k is odd. For uniform meshes, the classical DG scheme with the central flux does have the optimal convergence rate $k+1$, observed in the numerical experiments and proved theoretically under the condition that the number of cells in the mesh is *odd* [1, 15]. In this paper, we provide a new proof which is available for arbitrary number of cells and dimensions for linear hyperbolic equations. We have used the shifting technique [13, 14] to construct the special local projection to obtain the optimal error estimate on uniform meshes. We also numerically find the superconvergence phenomenon for the cell averages and numerical fluxes.

The outline of the paper is as follows. In section 2, we review the DG scheme for hyperbolic equations with central fluxes and give the error estimates for the semi-discrete version in one dimension. We extend our analysis to multi-dimensions in section 3. In section 4, we give numerical examples to show the sub-optimal convergence for non-uniform meshes and optimal convergence for uniform meshes in both one and two-dimensional cases. Finally, we give concluding remarks in section 5. Some of the technical proof of the lemmas and propositions is included in the Appendix A.

2. One Dimensional Problems

We consider the following one dimensional linear hyperbolic equation

$$\begin{cases} u_t + u_x = 0, & x \in [0,1],\ t \geq 0 \\ u(x,0) = u_0(x), & x \in [0,1], \end{cases} \tag{2.1}$$

with periodic boundary condition. We first introduce the usual notations of the DG method. For a given interval $\Omega = [0,1]$ and the index set $\mathbb{Z}_N = \{1, 2, \ldots, N\}$, the usual DG mesh $\mathcal{I}_N$ is defined as:

$$0 = x_{\frac{1}{2}} < x_{\frac{3}{2}} < \ldots < x_{N+\frac{1}{2}} = 1. \tag{2.2}$$

We denote

$$I_j = (x_{j-\frac{1}{2}}, x_{j+\frac{1}{2}}), \quad x_j = \frac{1}{2}(x_{j-\frac{1}{2}} + x_{j+\frac{1}{2}}), \quad h_j = x_{j+\frac{1}{2}} - x_{j-\frac{1}{2}}, \quad j \in \mathbb{Z}_N. \tag{2.3}$$

We also assume the mesh is regular, i.e., the ratio between the maximum and minimum mesh sizes shall stay bounded during mesh refinements. That means there exists a positive constant $\sigma \geq 1$, such that,

$$\frac{1}{\sigma}h \le h_j \le \sigma h, \quad h = \frac{1}{N}, \quad \forall j \in \mathbb{Z}_N. \tag{2.4}$$

We define the approximation space as

$$V_h^k = \{v_h : (v_h)|_{I_j} \in \mathbb{P}^k(I_j), j = 1, \ldots, N\}. \tag{2.5}$$

Here $\mathbb{P}^k(I_j)$ denotes the set of all polynomials of degree at most k on I_j. We first introduce some standard Sobolev space notations. For any integer $m > 0$, $W^{m,p}(D)$ denote the standard Sobolev spaces on the sub-domain $D \subset \Omega$ equipped with the norm $\|\cdot\|_{m,p,D}$ and the semi-norm $|\cdot|_{m,p,D}$. If $p = 2$, we set $W^{m,p}(D) = H^m(D)$, and $|\cdot|_{m,p,D} = |\cdot|_{m,D}$ and we omit the index D, when $D = \Omega$.

The semi-discrete DG scheme is to seek $u_h \in V_h$ such that for all $v_h \in V_h$,

$$((u_h)_t, v_h)_j + a_j(u_h, v_h) = 0, \quad \forall j \in \mathbb{Z}_N, \tag{2.6}$$

where

$$a_j(u_h, v_h) = -(u_h, (v_h)_x)_j + \hat{u_h} v_h^-|_{j+\frac{1}{2}} - \hat{u_h} v_h^+|_{j-\frac{1}{2}}, \tag{2.7}$$

where $(u, v)_j = \int_{I_j} uv\, dx$, $v^-|_{j+\frac{1}{2}}$ and $v^+|_{j+\frac{1}{2}}$ denote the left and right limits of v at the point $x_{j+\frac{1}{2}}$, respectively, and $\hat{u_h}$ are the numerical fluxes. Here, we consider the central flux,

$$\hat{u_h} = \{u_h\} = \frac{1}{2}(u_h^- + u_h^+). \tag{2.8}$$

For the central flux, we have,

$$\sum_{j=1}^{N} a_j(u_h, u_h) = 0, \quad \forall u_h \in V_h. \tag{2.9}$$

The initial datum $u_h(x, 0) = Pu_0$ is obtained by the standard L^2 projection,

$$(u_0 - Pu_0, v_h)_j = 0, \quad \forall v_h \in \mathbb{P}^k(I_j). \tag{2.10}$$

Thus, we have,

$$\|u_0 - u_h(\cdot, 0)\| \lesssim h^{k+1}\|u\|_{k+1}. \tag{2.11}$$

Here and below, an unmarked norm $\|\cdot\|$ denotes the L^2 norm, and $A \lesssim B$ denotes that A can be bounded by B multiplied by a constant independent of the mesh size h. As mentioned earlier, we have the following energy-conserving results [15].

Theorem 2.1. *Suppose u_h is the solution of DG scheme* (2.6)*, then it satisfies*

$$\frac{d}{dt}\|u_h\|^2 = 0. \tag{2.12}$$

Next we consider the error estimate, first we recall the following basic facts [5]. For any function $w_h \in V_h$,

$$(i) \quad \|(w_h)_x\| \lesssim h^{-1}\|w_h\|, \tag{2.13a}$$

$$(ii) \quad \|w_h\|_{\Gamma_h} \lesssim h^{-\frac{1}{2}}\|w_h\|, \tag{2.13b}$$

where Γ_h denotes the set of boundary points of all elements I_j, and the norm

$$\|w_h\|_{\Gamma_h} = \left(\sum_{j=1}^{N} ((w_h)^+_{j+\frac{1}{2}})^2 + ((w_h)^-_{j-\frac{1}{2}})^2 \right)^{\frac{1}{2}}.$$

In order to obtain the optimal error estimate for the case of uniform meshes, we need to use the shifting technique [13, 14] to construct a special projection $P_h^\star$, which is defined as follows. For any given function $w \in L^\infty(\Omega)$ and each j,

$$\int_{I_j} P_h^\star w(x)\, dx = \int_{I_j} w(x)\, dx, \tag{2.14}$$

$$\widetilde{P_h}(P_h^\star w; v)_j = \widetilde{P_h}(w; v)_j, \qquad \forall v \in \mathbb{P}^k(I_j), \tag{2.15}$$

where $\widetilde{P_h}(w; v)_j$ is defined as

$$\widetilde{P_h}(w; v)_j = -(w, v_x)_j + \frac{w(x^-_{j+\frac{1}{2}}) + w(x^+_{j-\frac{1}{2}})}{2} \Big(v(x^-_{j+\frac{1}{2}}) - v(x^+_{j-\frac{1}{2}}) \Big). \tag{2.16}$$

Note that the projection $P_h^\star$ is a local projection, so we only consider the projection defined on the reference interval $[-1, 1]$. We have the following lemma to establish the fact that the projection is well defined.

Lemma 2.1. *When k is even, the projection $P_h^\star$ defined by* (2.14) *on the interval $[-1, 1]$ exists and is unique for any L^∞ function w, and the projection is bounded in the L^∞ norm, i.e.,*

$$\|P_h^\star w\|_\infty \le C(k)\|w\|_\infty, \tag{2.17}$$

where $C(k)$ is a constant that only depends on k but is independent of w.

Proof. We provide the proof of this lemma in the appendix; see section A.1. □

Remark 2.1. The projection $P_h^\star$ is only well defined when k is even. In fact, when k is odd, for example $k = 1$, we can take $w_I = x \in \mathbb{P}^1([-1, 1])$, which satisfies

$$\int_{-1}^{1} w_I(x)\, dx = 0, \tag{2.18}$$

$$\widetilde{P_h}(w_I; v) = -\int_{-1}^{1} w_I(x) v_x\, dx + \frac{w_I(1) + w_I(-1)}{2}(v(1) - v(-1)) = 0, \qquad \forall v \in \mathbb{P}^1([-1, 1]). \tag{2.19}$$

It means that there exists a nonzero function $w_I = P_h^\star w$, where $w \equiv 0$. This implies that $P_h^\star w$ is not unique.

Remark 2.2. In fact, the projection $P_h^\star$ has an equivalent definition as follows,

$$\int_{x_{j-\frac{1}{2}}}^{x_{j+\frac{1}{2}}} P_h^\star w v\, dx = \int_{x_{j-\frac{1}{2}}}^{x_{j+\frac{1}{2}}} w v\, dx, \qquad \forall v \in \mathbb{P}^{k-1}(I_j), \tag{2.20}$$

$$\frac{1}{2}\Big(P_h^\star w(x^-_{j+\frac{1}{2}}) + P_h^\star w(x^+_{j-\frac{1}{2}}) \Big) = \frac{1}{2}\Big(w(x_{j+\frac{1}{2}}) + w(x_{j-\frac{1}{2}}) \Big). \tag{2.21}$$

As a direct corollary of lemma 2.1 and the locality of the projection, the standard approximation theory [5] implies, for a smooth function w,

$$\|P_h^\star w(x) - w(x)\| + h^{\frac{1}{2}} \|P_h^\star w(x) - w(x)\|_{\Gamma_h} \lesssim h^{k+1} \|w\|_{k+1}. \tag{2.22}$$

We also have the following properties of the projection $P_h^\star$,

Lemma 2.2. *Suppose that $u = x^{k+1}$. Let $u_j = P_h^\star u|_{I_j}$. If $h_{j-1} = h_j = h_{j+1} = h$, then we have the following relationship:*

$$(x-h)^{k+1} - u_{j-1}(x-h) = x^{k+1} - u_j(x) = (x+h)^{k+1} - u_{j+1}(x+h), \quad \forall x \in I_j. \tag{2.23}$$

where $P_h^\star u|_{I_j}$ means that the projection of u is defined on the subinterval I_j, and $u_{j-1}(x-h)$, $u_{j+1}(x+h)$ refer to the projection of u on the element I_{j-1} and I_{j+1} respectively, since $x \in I_j$ implies $(x-h) \in I_{j-1}$ and $(x+h) \in I_{j+1}$.

Proof. The proof of this lemma is based on the same arguments as in [13, 14], so we omit it here. □

By this lemma, we also have the following superconvergence results.

Proposition 2.1. *Given the index j, suppose that u is a $(k+1)$th degree polynomial function in $\mathbb{P}^{k+1}(I_{j-1} \bigcup I_j \bigcup I_{j+1})$. If $h_{j-1} = h_j = h_{j+1} = h$, we have*

$$a_j(P_h^\star u, v_h) = a_j(u, v_h) \quad \forall v_h \in \mathbb{P}^k(I_j), \tag{2.24}$$

where a_j is defined by (2.7).

Then we can state the main theorem of this paper.

Theorem 2.2. *Suppose u_h is the numerical solution of the DG scheme* (2.6) *for equation* (2.1) *with a smooth initial condition $u(\cdot, 0) \in H^{k+2}(\Omega)$, and u is the exact solution of* (2.1)*, then the approximation u_h satisfies the following L^2 error estimate:*

$$\|u(\cdot, T) - u_h(\cdot, T)\| \lesssim h^k, \tag{2.25}$$

where k is the degree of the piecewise polynomials in the finite element spaces V_h. Furthermore, when k is even and the mesh is uniform, we have the optimal error estimate:

$$\|u(\cdot, T) - u_h(\cdot, T)\| \lesssim h^{k+1}. \tag{2.26}$$

Proof. Obviously, the exact solution u of (2.1) also satisfies

$$(u_t, v_h) + a_j(u, v_h) = 0, \quad \forall v_h \in V_h. \tag{2.27}$$

Subtracting (2.6) from (2.27), we obtain the error equation

$$((u - u_h)_t, v_h)_j + a_j(u - u_h, v_h) = 0, \quad \forall v_h \in V_h. \tag{2.28}$$

We denote

$$\xi = u_h - P^\star u; \quad \eta = u - P^\star u, \tag{2.29}$$

where $P^\star$ is some projection. From the error equation (2.28), and taking $v_h = \xi$, we have

$$(\xi_t, \xi)_j + a_j(\xi, \xi) = (\eta_t, \xi)_j + a_j(\eta, \xi). \tag{2.30}$$

For the nonuniform mesh case, the sub-optimal error estimate can be easily obtained by using the standard L^2 projection P. We take $P^\star$ as the standard L^2 projection P, then we have,

$$\|u - Pu\| + h^{\frac{1}{2}}\|u - Pu\|_{\Gamma_h} \lesssim h^{k+1}\|u\|_{k+1}. \tag{2.31}$$

For the left-hand side of (2.30), we can use (2.9) to obtain

$$\frac{1}{2}\frac{d}{dt}\|\xi\|^2 = -\sum_{j=1}^{N}\{\eta\}_{j+\frac{1}{2}}[\xi]_{j+\frac{1}{2}} \lesssim h^k\|\xi\|\|u\|_{k+1}, \tag{2.32}$$

where the last inequality is from (2.31) and (ii) of (2.13a). Thus, by using Gronwall's inequality and (2.11), we have,

$$\|\xi\| \lesssim h^k\|u\|_{k+1}. \tag{2.33}$$

The triangle inequality implies our designed results for the general non-uniform mesh case.

For the case of uniform meshes, when k is even, we take $P^\star$ as $P_h^\star$ which is defined in (2.14). Let u_I^j be the Taylor expansion polynomial of order $k+1$ of u over $D_j = (x_{j-\frac{3}{2}}, x_{j+\frac{3}{2}})$, i.e., $u_I^j(x) = \sum_{i=0}^{k+1} u^{(i)}(x_j)(x - x_j)^i$, $x \in D_j$. Let r_u^j denote the remainder term, i.e., $r_u^j = u - u_I^j$. Recalling the Bramble-Hilbert lemma in [5], we have

$$\|r_u^j\|_{L^\infty(D_j)} \lesssim h^{k+\frac{3}{2}}|u|_{k+2,D_j}. \tag{2.34}$$

Thus, using Proposition 2.1, we have

$$\begin{aligned} a_j(\eta, \xi) &= a_j(u_I^j - P_h^\star u_I^j, \xi) + a_j(r_u^j - P_h^\star r_u^j, \xi) \\ &= a_j(r_u^j - P_h^\star r_u^j, \xi). \end{aligned}$$

By using the property of the projection (2.17) and (2.34), and the inverse inequality in (2.13a) for ξ, we have

$$\sum_j a_j(\eta, \xi) \lesssim h^{2k+2}\|u\|_{k+2} + \|\xi\|^2. \tag{2.35}$$

Therefore, form (2.30), (2.22) and the stability result (2.1), we have

$$\frac{1}{2}\frac{d}{dt}\|\xi\|^2 \lesssim h^{2k+2}\|u\|_{k+2} + \|\xi\|^2. \tag{2.36}$$

This together with the approximation results (2.22) and the initial datum (2.11), implies the desired error estimate (2.26). □

We summarize the theoretical findings and numerical findings in Table 2.1.

From Table 2.1, we can see that our theoretical findings are sharp and consistent with the numerical results. We emphasize that when k is even, in order to produce the sub-optimal accuracy, we have designed a special regular mesh sequence which is motivated by [11], see section 4.

Table 2.1: Summarization of the L^2 error accuracy for the 1D case.

	mesh	k is odd	k is even
Numerically	uniform	kth	$(k+1)$th
	non-uniform		kth
Theoretically	uniform	kth	$(k+1)$th
	non-uniform		kth

3. Multi-dimensional Problems

In this section, we consider the semidiscrete DG method with central fluxes for multidimensional linear hyperbolic equations. Without loss of generality, we only study the two dimensional problem; all the arguments we present in our analysis depends on the tensor product structure of the mesh and the finite element space and can be easily extended to the more general cases $d > 2$. Hence, we consider the following two-dimensional problem

$$\begin{cases} u_t + u_x + u_y = 0, & (x, y, t) \in \Omega \times (0, T], \\ u(x, y, 0) = u_0(x, y), & (x, y) \in \Omega. \end{cases} \tag{3.1}$$

again with periodic boundary conditions. Without loss of generality, we assume $\Omega = [0, 1]^2$. We use the regular Cartesian mesh,

$$\left\{ K_{i,j} = I_i \times J_j = [x_{i-\frac{1}{2}}, x_{i+\frac{1}{2}}] \times [y_{j-\frac{1}{2}}, y_{j+\frac{1}{2}}] \right\}, \quad i = 1, \ldots, N_x, \;\; j = 1, \ldots, N_y.$$

We denote $h_x^i = x_{i+\frac{1}{2}} - x_{i-\frac{1}{2}}$, $h_y^j = y_{j+\frac{1}{2}} - y_{j-\frac{1}{2}}$ and $h = \max_{i,j}(h_x^i, h_y^j)$. Let $W_h := \{v \in L^2(\Omega) : v|_{K_{i,j}} \in \mathbb{Q}^k(K_{i,j}), \forall i, j\}$, where $\mathbb{Q}^k(K_{i,j})$ denotes the space of tensor-product polynomials of degrees at most k in each variable defined on $K_{i,j}$.

The semidiscrete DG scheme with central fluxes is as follows. We seek $u_h \in W_h$, such that for all test functions $v \in W_h$, and all i, j,

$$\begin{aligned} \int_{K_{i,j}} (u_h)_t v \, dxdy = & \int_{K_{i,j}} (u_h v_x + u_h v_y) \, dxdy \\ & - \int_{y_{j-\frac{1}{2}}}^{y_{j+\frac{1}{2}}} \left(\hat{u}_h(x_{i+\frac{1}{2}}, y) v(x^-_{i+\frac{1}{2}}, y) - \hat{u}_h(x_{i-\frac{1}{2}}, y) v(x^+_{i-\frac{1}{2}}, y) \right) dy \\ & - \int_{x_{i-\frac{1}{2}}}^{x_{i+\frac{1}{2}}} \left(\tilde{u}_h(x, y_{j+\frac{1}{2}}) v(x, y^-_{j+\frac{1}{2}}) - \tilde{u}_h(x, y_{j-\frac{1}{2}}) v(x, y^+_{j-\frac{1}{2}}) \right) dx \qquad (3.2) \\ =: & b_{i,j}(u_h, v), \qquad (3.3) \end{aligned}$$

where

$$\hat{u}_h(x_{i+\frac{1}{2}}, y) = \frac{u_h(x^+_{i+\frac{1}{2}}, y) + u_h(x^-_{i+\frac{1}{2}}, y)}{2}; \quad \tilde{u}_h(x, y_{j+\frac{1}{2}}) = \frac{u_h(x, y^+_{j+\frac{1}{2}}) + u_h(x, y^-_{j+\frac{1}{2}})}{2}. \tag{3.4}$$

For the initial data, we take $u_h(0) = Pu_0$, where P is the L^2 projection into W_h, and we have [5]

$$\|u_0 - Pu_0\| \lesssim h^{k+1} \|u_0\|_{k+1}. \tag{3.5}$$

We also have

$$\sum_{i=1}^{N_x}\sum_{j=1}^{N_y} b_{i,j}(u_h, u_h) = 0, \quad \forall u_h \in W_h. \tag{3.6}$$

Thus we have the following energy conservative property

Proposition 3.1. *The numerical solution of* (3.2) *satisfies*

$$\frac{1}{2}\frac{d}{dt}\|u_h\|^2 = 0. \tag{3.7}$$

3.1. A priori error estimates

Let us now state our main result as a theorem, whose proof will be provided in the next subsection.

Theorem 3.1. *Suppose u_h is the numerical solution of the DG scheme* (3.2) *for Eq.* (3.1) *with a smooth initial condition $u(x, y, 0) \in H^{k+2}(\Omega)$, and u is the exact solution of* (3.1)*, then the approximation u_h satisfies the following L^2 error estimate:*

$$\|u(x, y, T) - u_h(x, y, T)\| \lesssim h^k, \tag{3.8}$$

where k is the degree of the piecewise tensor-product polynomials in the finite element spaces W_h. Furthermore, when k is even and the mesh is uniform, we have the optimal error estimate,

$$\|u(x, y, T) - u_h(x, y, T)\| \lesssim h^{k+1}. \tag{3.9}$$

Remark 3.1. We note that the finite element space $V_h := \{v \in L^2(\Omega) : v|_{K_{i,j}} \in \mathbb{P}^k(K_{i,j}), \forall i, j\}$, where $\mathbb{P}^k(K_{i,j})$ denotes the space of polynomials of degrees at most k defined on $K_{i,j}$, can also be taken as the approximation space. But it only has the sub-optimal accuracy of order k in the numerical examples, see section 4. Thus, here we only consider the tensor product space.

By the same arguments as in the one dimensional problem, we also have the error equation

$$\int_{K_{i,j}} (u - u_h)_t v \, dxdy - b_{i,j}(u - u_h, v) = 0, \quad \forall v \in W_h, \forall i, j. \tag{3.10}$$

3.2. Proof of the error estimates

We divide the proof of Theorem 3.1 into several steps. First, for non-uniform meshes, the proof of the sub-optimal error estimate is straightforward. We just need to use the standard L^2 projection and follow the standard error estimates of DG methods which is the same as in the one dimensional case. Thus next we only consider the uniform mesh case. In order to prove the optimal error estimate when k is even, we need to construct the special local projection $\Pi_h^\star$. In addition, the optimal approximation properties of $\Pi_h^\star$ are derived. The superconvergence results of the special projections would be given in the subsection 3.2.2. Finally, we finish the proof of Theorem 3.1 in subsection 3.2.3.

3.2.1. The special projection $\Pi_h^\star$

Since our finite element space consists of piecewise $\mathbb{Q}^k$ polynomials, we use the tensor product technique to construct the 2D projection. We define $\Pi_h^\star$ as the following projection into W_h. For each $K_{i,j}$,

$$\int_{K_{i,j}} \Pi_h^\star w(x,y)v(x,y)\,dxdy = \int_{K_{i,j}} w(x,y)v(x,y)\,dxdy, \quad \forall v \in \mathbb{Q}^{k-1}(K_{i,j}). \tag{3.11a}$$

$$\int_{I_i} \frac{\Pi_h^\star w(x,y^-_{j+\frac{1}{2}})+\Pi_h^\star w(x,y^+_{j-\frac{1}{2}})}{2}\varphi(x)dx = \int_{I_i} \frac{w(x,y^-_{j+\frac{1}{2}})+w(x,y^+_{j-\frac{1}{2}})}{2}\varphi(x)dx, \quad \forall \varphi(x) \in \mathbb{P}^{k-1}(I_i), \tag{3.11b}$$

$$\int_{J_j} \frac{\Pi_h^\star w(x^-_{i+\frac{1}{2}},y)+\Pi_h^\star w(x^+_{i-\frac{1}{2}},y)}{2}\varphi(y)dy = \int_{J_j} \frac{w(x^-_{i+\frac{1}{2}},y)+w(x^+_{i-\frac{1}{2}},y)}{2}\varphi(y)dy, \quad \forall \varphi(y) \in \mathbb{P}^{k-1}(J_j), \tag{3.11c}$$

$$\begin{aligned}&\frac{1}{4}\left(\Pi_h^\star w(x^-_{i+\frac{1}{2}},y^-_{j+\frac{1}{2}}) + \Pi_h^\star w(x^-_{i+\frac{1}{2}},y^+_{j-\frac{1}{2}}) + \Pi_h^\star w(x^+_{i-\frac{1}{2}},y^-_{j+\frac{1}{2}}) + \Pi_h^\star w(x^+_{i-\frac{1}{2}},y^+_{j-\frac{1}{2}})\right)\\ &= \frac{1}{4}\left(w(x^-_{i+\frac{1}{2}},y^-_{j+\frac{1}{2}}) + w(x^-_{i+\frac{1}{2}},y^+_{j-\frac{1}{2}}) + \ w(x^+_{i-\frac{1}{2}},y^-_{j+\frac{1}{2}}) + w(x^+_{i-\frac{1}{2}},y^+_{j-\frac{1}{2}})\right).\end{aligned} \tag{3.11d}$$

Again, since the projection is local, we only consider the projection defined on the reference cell $[-1,1]\times[-1,1]$. We establish the existence and uniqueness of the projection when k is even in the following lemma

Lemma 3.1. *When k is even, the projection $\Pi_h^\star$ defined by* (3.11) *on the cell $[-1,1]\times[-1,1]$ exists and is unique for any L^∞ function w, and the projection is bounded in the L^∞ norm, i.e.*

$$\|\Pi_h^\star w\|_\infty \le C(k)\|w\|_\infty, \tag{3.12}$$

where $C(k)$ is a constant that only depends on k but is independent of w.

Proof. The proof of this lemma is given in the Appendix; see section A.2. □

Since the projection is a k-th degree polynomial preserving local projection, standard approximation theory [5] implies, for a smooth function w,

$$\|w - \Pi_h^\star w\|_{L^2(K_{i,j})} \lesssim h^{k+1}\|w\|_{k+1,K_{i,j}}. \tag{3.13}$$

For the two dimensional space, for any $\omega_h \in W_h$, the following inequalities hold,

$$\|\partial_x \omega_h\| \lesssim h^{-1}\|\omega_h\|, \qquad \|\omega_h\|_{L^2(\partial K_{i,j})} \lesssim h^{-1/2}\|\omega_h\|, \qquad \|\omega_h\|_\infty \lesssim h^{-1}\|\omega_h\|, \tag{3.14}$$

where $\partial K_{i,j}$ is the boundary of cell $K_{i,j}$.

Remark 3.2. By similar arguments as in the one dimensional problem, we note that the projection $\Pi_h^\star$ is not well defined when k is odd.

3.2.2. Properties of the projection $\Pi_h^\star$

By the similar arguments in the one dimensional case, we have the following lemma:

Lemma 3.2. *Assume that $u = x^{k+1}$ or y^{k+1}. Let $u_{i,j} = \Pi_h^\star u|_{K_{i,j}}$. If $h_x^{i-1} = h_x^i = h_x^{i+1} = h_x$ and $h_y^{j-1} = h_y^j = h_y^{j+1} = h_y$, then $\forall (x,y) \in K_{i,j}$, we have following relationship:*

$$\begin{aligned}&u(x-h_x,y) - u_{i-1,j}(x-h_x,y) = u(x,y) - u_{i,j}(x,y) = u(x+h_x) - u_{i+1,j}(x+h_x,y)\\ =&u(x,y+h_y) - u_{i,j+1}(x,y+h_y) = u(x,y-h_y) - u_{i,j-1}(x,y-h_y).\end{aligned} \tag{3.15}$$

Similar to the one dimensional case, we also have the following superconvergence result.

Proposition 3.2. *For a given index (i,j), suppose that u is a $(k+1)$th degree polynomial function in $\mathbb{P}^{k+1}(D_{i,j})$, where $D_{i,j} = K_{i-1,j} \bigcup K_{i+1,j} \bigcup K_{i,j} \bigcup K_{i,j-1} \bigcup K_{i,j+1}$. If $h_x^{i-1} = h_x^i = h_x^{i+1}$ and $h_y^{j-1} = h_y^j = h_y^{j+1}$, then we have*

$$b_{i,j}(\Pi_h^\star u, v) = b_{i,j}(u,v) \quad \forall v \in \mathbb{Q}^k(K_{i,j}), \tag{3.16}$$

where $b_{i,j}(\cdot,\cdot)$ is defined by (3.3).

Proof. We provide the proof of this Proposition in the Appendix; see section A.3. □

3.2.3. Proof of Theorem 3.1

Let

$$\xi = u_h - \Pi_h^\star u; \quad \eta = u - \Pi_h^\star u. \tag{3.17}$$

From (3.10), we obtain

$$\int_{K_{i,j}} (\xi)_t v \, dxdy - b_{i,j}(\xi, v) = \int_{K_{i,j}} (\eta)_t v \, dxdy - b_{i,j}(\eta, v), \quad \forall v \in \mathbb{Q}^k(K_{i,j}). \tag{3.18}$$

Take $v = \xi \in W_h$, for the left hand side of (3.18), we use (3.6) to obtain

$$\sum_{i,j} \int_{K_{i,j}} (\xi)_t \xi \, dxdy - b_{i,j}(\xi,\xi) = \frac{1}{2}\frac{d}{dt}\|\xi\|^2. \tag{3.19}$$

For each element $K_{i,j}$, we consider the Taylor expansion of u around (x_i, y_j):

$$u = Tu + Ru, \tag{3.20}$$

where

$$Tu = \sum_{l=0}^{k+1} \sum_{m=0}^{l} \frac{1}{(l-m)!m!} \frac{\partial^l u(x_i, y_j)}{\partial x^{l-m} \partial y^m} (x - x_i)^{l-m} (y - y_j)^m,$$

$$Ru = (k+2) \sum_{m=0}^{k+2} \frac{(x - x_i)^{k+2-m}(y - y_j)^m}{(k+2-m)!m!} \int_0^1 (1-s) \frac{\partial^{k+2} u(x_i^s, y_j^s)}{\partial x^{k+2-m} \partial y^m} \, ds,$$

with $x_i^s = x_i + s(x - x_i)$, $y_j^s = y_j + s(y - y_j)$. Clearly, $Tu \in \mathbb{P}^{k+1}(D_{i,j})$. By the linearity of the projection, and from (3.16), we then get

$$\begin{aligned} b_{i,j}(\eta, v) &= b_{i,j}(Tu - \Pi_h^\star Tu, v) + b_{i,j}(Ru - \Pi_h^\star Ru, v) \\ &= b_{i,j}(Ru - \Pi_h^\star Ru, v). \end{aligned} \tag{3.21}$$

Again recalling the Bramble-Hilbert lemma in [5] , we have

$$\|Ru\|_{L^\infty(D_{i,j})} \leq C h^{k+1} |u|_{H^{k+2}(D_{i,j})}. \tag{3.22}$$

Table 3.1: Summarization of the L^2 error accuracy for the 2D case.

		mesh	k is odd	k is even
$\mathbb{Q}^k$-space	Numerically	uniform	kth	$(k+1)$th
		non-uniform		kth
	Theoretically	uniform	kth	$(k+1)$th
		non-uniform		kth
$\mathbb{P}^k$-space	Numerically/Theoretically	uniform/nonuniform	kth	kth

Thus, this together with the standard approximate proposition of the projection (3.13), and the inverse inequality in (3.14) for ξ, we have

$$\sum_{i,j} b_{i,j}(\eta,\xi) \lesssim h^{2k+2}\|u\|_{k+2}^2 + \|\xi\|^2. \tag{3.23}$$

From (3.19), (3.23) and (3.18), we have

$$\frac{1}{2}\frac{d}{dt}\|\xi\|^2 \lesssim h^{2k+2}\|u\|_{k+2}^2 + \|\xi\|^2. \tag{3.24}$$

This together with the approximation results (3.13) and the initial discretization (3.5), implies the desired error estimate (3.9). □

To end this section, we summarize our theoretical findings and numerical findings for the 2D problem in Table 3.1. Again our theoretical proof is sharp and consistent with the numerical results.

4. Numerical Examples

In this section, we present some numerical examples to verify our theoretical findings. In our numerical experiments, we present the E_2, E_A, and E_f errors, respectively. They are defined by

$$E_2 = \|u - u_h\|. \tag{4.1}$$

$$E_A = \begin{cases} \left(\dfrac{1}{N}\displaystyle\sum_{j=1}^{N}\left(\frac{1}{h_j}\int_{I_j}(u-u_h)\,dx\right)^2\right)^{\frac{1}{2}}, & \text{for one dimension,} \\ \left(\dfrac{1}{N_xN_y}\displaystyle\sum_{j=1}^{N_y}\sum_{i=1}^{N_x}\left(\frac{1}{h_x^i h_y^j}\int_{K_{i,j}}(u-u_h)\,dxdy\right)^2\right)^{\frac{1}{2}}, & \text{for two dimensions.} \end{cases} \tag{4.2}$$

$$E_f = \left(\frac{1}{N}\sum_{j=1}^{N}(u_{j+\frac{1}{2}} - \{u_h\}_{j+\frac{1}{2}})^2\right)^{\frac{1}{2}}. \tag{4.3}$$

Example 4.1. We consider the linear hyperbolic equation with periodic boundary condition:

$$\begin{cases} u_t + u_x = 0, \qquad (x,t) \in [0,2\pi]\times(0,T), \\ u(x,0) = \exp(\sin(x)), \\ u(0,t) = u(2\pi,t). \end{cases} \tag{4.4}$$

The exact solution to this problem is

$$u(x,t) = \exp(\sin(x-t)). \tag{4.5}$$

We use two kinds of non-uniform meshes. The first one is the non-uniform mesh with 30% random perturbation from N uniform cells on $[0,2\pi]$, and the other mesh is constructed as follows. Let $\tilde{x}_{j+\frac{1}{2}} = jh$ for $j = 0,\ldots,N$ where $h = \frac{2\pi}{N}$ and $\tilde{x}_{N+\frac{1}{2}} = 1$, then we define the nodes of our mesh as follows

$$x_{2j-\frac{1}{2}} = \tilde{x}_{2j-\frac{1}{2}} + \alpha h, \quad j = 1,\ldots,\lfloor N/2 \rfloor.$$

Table 4.1: The errors and corresponding convergence rates for the DG with $k = 0, 2, 4$ in 1D. The terminal time $T = 1$ and the parameter of the mesh $\alpha = 0.1$.

	N	E_2	Rate	E_A	Rate	E_f	Rate
$k = 0$	10	5.14E-01	–	1.23E-01	–	1.15E-01	–
	20	2.75E-01	0.90	7.32E-02	0.75	3.20E-02	1.85
	40	2.02E-01	0.44	6.98E-02	0.07	7.66E-03	2.06
	80	1.82E-01	0.15	7.01E-02	-0.01	5.75E-03	0.41
	160	1.77E-01	0.04	7.03E-02	-0.00	6.45E-03	-0.16
	320	1.75E-01	0.01	7.03E-02	-0.00	6.68E-03	-0.05
	640	1.75E-01	0.00	7.03E-02	-0.00	6.75E-03	-0.01
	1280	1.75E-01	0.00	7.04E-02	-0.00	6.76E-03	-0.00
	2560	1.75E-01	0.00	7.04E-02	-0.00	6.77E-03	-0.00
	5120	1.75E-01	0.00	7.04E-02	-0.00	6.77E-03	-0.00
	LS order		0.12		0.05		0.32
$k = 2$	10	9.30E-03	–	1.09E-03	–	2.07E-03	–
	20	7.82E-04	3.57	8.21E-05	3.73	2.20E-04	3.23
	40	1.33E-04	2.55	9.77E-06	3.07	2.10E-05	3.39
	80	2.00E-05	2.73	9.26E-07	3.40	2.19E-06	3.26
	160	4.21E-06	2.25	1.21E-07	2.94	2.36E-07	3.22
	320	9.99E-07	2.07	2.10E-08	2.52	1.48E-08	4.00
	640	2.46E-07	2.02	1.98E-09	3.41	3.35E-09	2.14
	1280	6.13E-08	2.01	3.37E-10	2.55	8.36E-11	5.32
	2560	1.53E-08	2.00	4.64E-12	6.18	7.30E-11	0.20
	5120	3.83E-09	2.00	1.14E-12	2.03	8.80E-12	3.05
	LS order		2.28		3.27		3.17
$k = 4$	10	1.21E-04	–	2.18E-06	–	1.61E-05	–
	20	1.62E-06	6.22	6.45E-08	5.08	6.56E-07	4.62
	40	9.60E-08	4.08	2.82E-09	4.51	1.41E-08	5.53
	80	5.28E-09	4.19	1.50E-10	4.24	4.13E-10	5.10
	160	3.22E-10	4.04	1.72E-12	6.44	1.64E-11	4.65
	320	1.99E-11	4.02	8.17E-14	4.40	2.34E-13	6.13
	640	1.24E-12	4.00	3.41E-16	7.90	1.81E-14	3.69
	1280	7.75E-14	4.00	3.18E-17	3.42	4.93E-16	5.19
	2560	4.85E-15	4.00	1.27E-18	4.64	1.59E-17	4.95
	5120	3.03E-16	4.00	5.35E-20	4.57	4.69E-19	5.08
	LS order		4.16		5.14		5.00

where $\lfloor m \rfloor$ denotes the maximal integer no more than m. Here the parameter α satisfies $-1 < \alpha < 1$. For example, if $\alpha = 0$ then the resulting mesh is uniform.

We set the number of subintervals, $N = 2^i \times 10, i = 0, \ldots, 9$, in our experiments. We use the DG scheme (2.6) with central fluxes using $\mathbb{P}^k$ polynomials with $k = 0, 2, 4$. The initial datum is obtained by the standard L^2 projection. To reduce the time discretization error, the seventh-order strong stability-preserving Runge-Kutta method [10] with the time step $\Delta t = 0.01h$ is used. The errors and corresponding convergence rates for the special nonuniform mesh with $\alpha = 0.1$, the uniform mesh, and random perturbation mesh are separately listed in the Tables 4.1-4.3. Since the convergence rates have oscillations, especially for E_A and E_f, we have used

Table 4.2: The errors and corresponding convergence rates for the DG with $k = 0, 2, 4$ using the uniform mesh in 1D. The terminal time $T = 1$.

	N	E_2	Rate	E_A	Rate	E_f	Rate
$k = 0$	10	4.82E-01	–	1.07E-01	–	1.22E-01	–
	20	2.16E-01	1.16	3.06E-02	1.80	3.53E-02	1.79
	40	1.03E-01	1.07	7.91E-03	1.95	9.16E-03	1.95
	80	5.09E-02	1.02	1.99E-03	1.99	2.31E-03	1.99
	160	2.54E-02	1.01	4.99E-04	2.00	5.79E-04	2.00
	320	1.27E-02	1.00	1.25E-04	2.00	1.45E-04	2.00
	640	6.34E-03	1.00	3.12E-05	2.00	3.62E-05	2.00
	1280	3.17E-03	1.00	7.81E-06	2.00	9.06E-06	2.00
	2560	1.58E-03	1.00	1.95E-06	2.00	2.27E-06	2.00
	5120	7.92E-04	1.00	4.88E-07	2.00	5.66E-07	2.00
	LS order		1.02		1.98		1.98
$k = 2$	10	9.11E-03	–	1.27E-03	–	2.50E-03	–
	20	5.47E-04	4.06	1.78E-05	6.15	8.32E-05	4.91
	40	6.12E-05	3.16	5.25E-07	5.08	3.13E-06	4.73
	80	7.52E-06	3.03	1.23E-08	5.42	3.41E-07	3.20
	160	9.32E-07	3.01	3.29E-10	5.22	2.44E-08	3.81
	320	1.16E-07	3.00	1.45E-11	4.50	3.58E-10	6.09
	640	1.45E-08	3.00	1.84E-13	6.31	1.27E-10	1.50
	1280	1.82E-09	3.00	1.08E-14	4.08	5.42E-12	4.55
	2560	2.27E-10	3.00	4.23E-16	4.68	1.35E-13	5.32
	5120	2.84E-11	3.00	6.77E-18	5.97	2.95E-14	2.20
	LS order		3.08		5.18		4.04
$k = 4$	10	1.18E-04	–	1.56E-06	–	2.03E-05	–
	20	1.03E-06	6.84	2.28E-08	6.09	3.13E-07	6.02
	40	2.76E-08	5.22	1.27E-10	7.49	5.78E-09	5.76
	80	8.11E-10	5.09	1.83E-12	6.11	8.19E-11	6.14
	160	2.49E-11	5.03	4.99E-15	8.52	1.94E-12	5.40
	320	7.78E-13	5.00	2.19E-17	7.83	2.71E-14	6.16
	640	2.43E-14	5.00	1.71E-19	7.00	3.79E-16	6.16
	1280	7.59E-16	5.00	5.35E-21	5.00	2.06E-18	7.53
	2560	2.37E-17	5.00	2.05E-23	8.03	1.20E-19	4.10
	5120	7.41E-19	5.00	6.25E-26	8.35	1.50E-21	6.32
	LS order		5.14		7.15		5.98

the least square method to fit the convergence orders of the errors, denoted by "LS order" in the tables. We can find that E_2 only has k-th order accuracy, but E_A and E_f have $(k+1)$-th order convergence for $k = 2, 4$, when the parameter of mesh $\alpha = 0.1$. For the uniform mesh, i.e., $\alpha = 0$, we observe the $(k+1)$-th optimal convergence rates. We can also find the convergence rates of the L^2 errors to be around $k + \frac{1}{2}$ for the randomly perturbed meshes.

In two dimensions, we consider the following problem.

Example 4.2. We solve the following linear hyperbolic equation with periodic boundary con-

Table 4.3: The errors and corresponding convergence rates for the DG with $k = 0, 2, 4$ using random perturbation mesh in 1D. The terminal time $T = 1$.

	N	E_2	Rate	E_A	Rate	E_f	Rate
$k = 0$	10	6.99E-01	–	2.30E-01	–	1.48E-01	–
	20	9.78E-01	-0.48	4.30E-01	-0.90	1.82E-01	-0.30
	40	3.06E-01	1.68	1.16E-01	1.89	4.26E-02	2.10
	80	2.90E-01	0.08	1.12E-01	0.05	2.54E-02	0.75
	160	1.63E-01	0.83	6.49E-02	0.79	1.48E-02	0.78
	320	1.74E-01	-0.10	6.99E-02	-0.11	1.39E-02	0.09
	640	8.47E-02	1.04	3.37E-02	1.05	5.15E-03	1.43
	1280	6.77E-02	0.32	2.69E-02	0.33	2.96E-03	0.80
	2560	5.35E-02	0.34	2.14E-02	0.33	2.08E-03	0.51
	5120	2.71E-02	0.98	1.08E-02	0.98	1.01E-03	1.04
	LS order		0.53		0.52		0.83
$k = 2$	10	2.73E-02	–	1.89E-03	–	6.94E-03	–
	20	7.18E-03	1.93	1.72E-04	3.46	4.07E-04	4.09
	40	1.05E-03	2.78	1.46E-05	3.55	3.14E-05	3.70
	80	1.10E-04	3.24	4.44E-06	1.72	7.56E-06	2.05
	160	3.27E-05	1.75	4.76E-07	3.22	8.11E-07	3.22
	320	4.21E-06	2.96	7.29E-08	2.71	1.16E-07	2.81
	640	1.00E-06	2.07	1.07E-08	2.77	1.67E-08	2.80
	1280	8.97E-08	3.48	1.52E-09	2.81	2.12E-09	2.98
	2560	3.12E-08	1.52	1.99E-10	2.93	2.52E-10	3.07
	5120	6.36E-09	2.29	2.80E-11	2.83	3.52E-11	2.84
	LS order		2.51		2.83		2.98
$k = 4$	10	2.28E-04	–	7.01E-06	–	3.73E-05	–
	20	7.81E-06	4.87	3.74E-07	4.23	1.92E-06	4.28
	40	2.72E-07	4.84	6.81E-09	5.78	3.37E-08	5.83
	80	1.53E-08	4.15	3.41E-10	4.32	1.71E-09	4.31
	160	1.57E-09	3.29	1.34E-11	4.66	6.94E-11	4.62
	320	7.00E-11	4.48	3.46E-13	5.28	1.38E-12	5.65
	640	5.60E-12	3.65	1.43E-14	4.59	5.33E-14	4.70
	1280	7.04E-14	6.31	4.29E-16	5.06	1.57E-15	5.09
	2560	1.88E-15	5.23	1.70E-17	4.66	5.10E-17	4.94
	5120	1.48E-16	3.66	5.87E-19	4.85	1.67E-18	4.93
	LS order		4.46		4.85		4.95

dition:

$$\begin{cases} u_t + u_x + u_y = 0, \quad (x, y, t) \in [0, 2\pi]^2 \times (0, T), \\ u(x, y, 0) = \sin(x + y). \end{cases} \tag{4.6}$$

The exact solution to this problem is

$$u(x, y, t) = \sin(x + y - 2t). \tag{4.7}$$

In each dimension, we apply the same partition as in the one-dimensional case. We choose the parameters $\alpha = 0.3$ (see Fig 5.1). The tensor product space $\mathbb{Q}^k$ or the piecewise kth

polynomial $\mathbb{P}^k$ is taken as the approximation space. We test the DG scheme with the central flux, and take the terminal time $T = 1$. When $\mathbb{Q}^k$ elements are used and $k = 0, 2$, for the special nonuniform mesh with $\alpha = 0.3$, the sub-optimal kth convergence rates can be observed which are listed in Table 4.4. For the uniform mesh, i.e., $\alpha = 0$, the scheme has $(k + 1)$th optimal convergence orders, see Table 4.5. However, for $\mathbb{P}^k$ finite element space, it only has kth suboptimal convergence rates no matter whether k is even or odd, see Table 4.6.

Table 4.4: The errors and corresponding convergence rates for the DG with $k = 0, 2$ in 2D. The terminal time $T = 1$ and the parameter of the mesh $\alpha = 0.3$.

	$N \times N$	E_2	Rate	E_A	Rate
$\mathbb{Q}^0$	4×4	3.67E+00	–	3.56E-01	–
	8×8	2.11E+00	0.80	2.34E-01	0.60
	16×16	1.74E+00	0.28	2.82E-01	-0.27
	32×32	1.67E+00	0.06	3.02E-01	-0.10
	64×64	1.66E+00	0.01	3.07E-01	-0.02
	128×128	1.65E+00	0.00	3.08E-01	-0.01
	LS order		0.20		-0.01
$\mathbb{Q}^2$	5×5	1.43E-01	–	4.08E-03	–
	9×9	4.28E-02	1.74	1.64E-03	1.32
	17×17	1.24E-02	1.78	3.06E-04	2.42
	33×33	3.33E-03	1.90	2.11E-05	3.85
	65×65	8.67E-04	1.94	3.12E-06	2.76
	129×129	2.21E-04	1.97	6.57E-07	2.25
	LS order		1.99		2.85

Table 4.5: The errors and corresponding convergence rates for the DG with $k = 0, 2$ using the uniform mesh in 2D. The terminal time $T = 1$.

	$N \times N$	E_2	Rate	E_A	Rate
$\mathbb{Q}^0$	4×4	3.65E+00	–	4.07E-01	–
	8×8	1.63E+00	1.17	1.34E-01	1.61
	16×16	7.43E-01	1.13	3.56E-02	1.91
	32×32	3.60E-01	1.04	9.04E-03	1.98
	64×64	1.79E-01	1.01	2.27E-03	1.99
	128×128	8.91E-02	1.00	5.68E-04	2.00
	LS order		1.07		1.92
$\mathbb{Q}^2$	4×4	1.99E-01	–	8.35E-03	–
	8×8	1.27E-02	3.97	7.97E-05	6.71
	16×16	1.21E-03	3.39	3.31E-06	4.59
	32×32	1.51E-04	2.99	1.85E-07	4.16
	64×64	1.88E-05	3.01	1.87E-09	6.63
	128×128	2.34E-06	3.01	1.17E-10	4.00
	LS order		3.23		5.16

Table 4.6: The errors and corresponding convergence rates for the DG with $k = 0, 2$ using random perturbation mesh in 2D. The terminal time $T = 1$.

	$N \times N$	E_2	Rate	E_A	Rate
$\mathbb{Q}^0$	4×4	3.76E+00	–	3.80E-01	–
	8×8	1.78E+00	1.08	1.55E-01	1.30
	16×16	1.23E+00	0.53	1.56E-01	-0.01
	32×32	8.83E-01	0.48	1.31E-01	0.25
	64×64	7.05E-01	0.33	1.07E-01	0.30
	128×128	5.63E-01	0.32	8.85E-02	0.28
	LS order		0.52		0.35
$\mathbb{Q}^2$	4×4	4.62E-01	–	1.17E-02	–
	8×8	3.22E-02	3.84	1.31E-03	3.15
	16×16	1.04E-02	1.64	1.98E-04	2.73
	32×32	2.06E-03	2.33	2.23E-05	3.15
	64×64	3.34E-04	2.63	2.93E-06	2.93
	128×128	3.56E-05	3.23	4.41E-07	2.74
	LS order		2.58		2.91

5. Concluding Remarks

In this paper, we have studied the error estimates of the DG methods for linear hyperbolic equations with central fluxes when the degree of piecewise polynomial is even. Numerically, we provide a counter example to show that the scheme only has the sub-optimal convergence rates for a particular regular non-uniform mesh sequence. Theoretically, we show that the scheme does have the optimal accuracy for uniform meshes in both one and multi-dimensional problems. Our proof does not have the constraint on the number of cells in the mesh. In numerical experiments, we have also observed that the superconvergence results for the errors of the cell averages and numerical fluxes. The theoretical proof of these superconvergence results would be interesting and challenging for our future work.

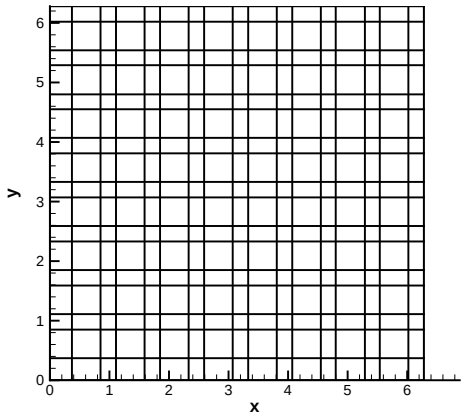

Fig. 5.1. Example of non-uniform two dimensional mesh with $h = \frac{2\pi}{17}$ and $\alpha = 0.3$

Table 5.1: The errors and corresponding convergence rates for the DG with using $\mathbb{P}^k$ finite element space in 2D. The terminal time $T = 1$ and the parameter of the mesh $\alpha = 0$.

	$N \times N$	E_2	Rate	E_A	Rate
$\mathbb{P}^1$	4×4	1.51E+00	–	7.53E-02	–
	8×8	6.88E-01	1.13	2.12E-02	1.83
	16×16	3.30E-01	1.06	5.77E-03	1.88
	32×32	1.63E-01	1.02	1.48E-03	1.96
	64×64	8.11E-02	1.01	3.72E-04	1.99
	128×128	4.05E-02	1.00	9.32E-05	2.00
$\mathbb{P}^2$	4×4	3.81E-01	–	7.83E-03	–
	8×8	6.31E-02	2.59	1.82E-03	2.11
	16×16	2.01E-02	1.65	7.97E-05	4.51
	32×32	5.31E-03	1.92	5.05E-06	3.98
	64×64	1.34E-03	1.98	3.29E-07	3.94
	128×128	3.37E-04	2.00	2.04E-08	4.01
$\mathbb{P}^3$	4×4	2.63E-01	1.93	1.30E-03	–
	8×8	7.84E-03	5.07	7.47E-05	4.12
	16×16	3.83E-04	4.35	3.63E-07	7.68
	32×32	3.39E-05	3.50	2.74E-08	3.73
	64×64	3.70E-06	3.19	4.84E-10	5.82
	128×128	4.46E-07	3.05	1.94E-11	4.64
	256×256	5.56E-08	3.01	9.59E-13	4.34

A. Appendix: Proof of a few technical lemmas and propositions

In this appendix, we provide the proof of some of the technical lemmas and propositions in the error estimates.

A.1. Proof of Lemma 2.1

Proof. Note that the procedure to find $P_h^\star w \in \mathbb{P}^k([-1,1])$ is to solve a linear system, so the existence and uniqueness are equivalent. Thus, we only prove the uniqueness of the projection $P_h^\star$. We set $w_I(x) = P_h^\star w(x)$ with $w(x) = 0$ and would like to prove $w_I(x) \equiv 0$. By the definition of the projection $P_h^\star w(x)$, then

$$\widetilde{P_h}(w_I; v) = -\int_{-1}^{1} w_I v_x \, dx + \frac{w_I(-1) + w_I(1)}{2}(v(1) - v(-1)) = 0, \quad \forall v \in \mathbb{P}^k([-1,1]), \quad \text{(A.1)}$$

$$\int_{-1}^{1} w_I \, dx = 0. \quad \text{(A.2)}$$

If $k = 0$, the lemma obviously holds. If $k \geq 2$, we take $v = x$ in (A.1), we have

$$0 = \widetilde{P_h}(w_I; x) = -\int_{-1}^{1} w_I \, dx + (w_I(-1) + w_I(1)) = (w_I(-1) + w_I(1)), \quad \text{(A.3)}$$

here we have used (A.2). Thus in (A.1), we have

$$0 = \widetilde{P_h}(w_I; v) = -\int_{-1}^{1} w_I v_x \, dx, \quad \forall v \in \mathbb{P}^k([-1,1]),$$

which means that

$$w_I = w_k L_k(x), \tag{A.4}$$

where w_k is a constant, and $L_k(x)$ is the standard k-th degree Legendre polynomial on the interval $[-1,1]$. By (A.3) and the fact that k is even, we obtain $w_k \equiv 0$. This finished the proof of uniqueness. For the proof of the bound (2.17), the arguments are the same as in [13, 14], hence we omit them here.

A.2. Proof of Lemma 3.1

Proof. When $k = 0$, the Lemma obviously holds true. For $k \geq 2$, assume that $u \equiv 0$. From (3.11a), we have $\Pi_h^\star u \perp \mathbb{Q}^{k-1}([-1,1]^2)$, thus we have the following expression of $\Pi_h^\star u$,

$$\Pi_h^\star u = \sum_{m=0}^{k-1} \alpha_{k,m} L_k(x) L_m(y) + \sum_{m=0}^{k-1} \alpha_{m,k} L_m(x) L_k(y) + \alpha_{k,k} L_k(x) L_k(y). \tag{A.5}$$

From (3.11b), we take $\varphi(x) = L_m(x)$, $m = 0, 1, \ldots, k-1$, to obtain

$$\alpha_{m,k} = 0, \quad m = 0, \ldots, k-1. \tag{A.6}$$

By the same arguments, we have

$$\alpha_{k,m} = 0, \quad m = 0, \ldots, k-1. \tag{A.7}$$

Thus $\Pi_h^\star u = \alpha_{k,k} L_k(x) L_k(y)$. Finally, by (3.11d) and the fact that k is even, we have $\alpha_{k,k} = 0$. That means $\Pi_h^\star u \equiv 0$. We have now finished the proof of uniqueness, hence also existence. By the same arguments as the proof of Lemma 2.1 in [14], we can obtain (3.12). □

A.3. Proof of Proposition 3.2

Proof. If $u \in \mathbb{Q}^k$, then $\Pi_h^\star u = u$ implies (3.16) holds true. Thus we only need to prove the cases $u = x^{k+1}$ or y^{k+1}. We will just show the details of the proof for one case; namely $b_{i,j}(\Pi_h^\star u, v) = b_{i,j}(u, v)$, $\forall v \in \mathbb{Q}^k(K_{i,j})$, is true when $u = x^{k+1}$. We denote $\Pi_e = \Pi_h^\star u - u$. By the definition of $b_{i,j}(\cdot,\cdot)$, we have

$$\begin{aligned} b_{i,j}(\Pi_e, v) = &\int_{K_{i,j}} \Pi_e v_x + \Pi_e v_y \, dxdy \\ &- \int_{J_j} \frac{\Pi_e(x^+_{i+\frac{1}{2}}, y) + \Pi_e(x^-_{i+\frac{1}{2}}, y)}{2} v(x^-_{i+\frac{1}{2}}, y) - \frac{\Pi_e(x^+_{i-\frac{1}{2}}, y) + \Pi_e(x^-_{i-\frac{1}{2}}, y)}{2} v(x^+_{i-\frac{1}{2}}, y)\, dy \\ &- \int_{I_i} \frac{\Pi_e(x, y^+_{j+\frac{1}{2}}) + \Pi_e(x, y^-_{j+\frac{1}{2}})}{2} v(x, y^-_{j+\frac{1}{2}}) - \frac{\Pi_e(x, y^+_{j-\frac{1}{2}}) + \Pi_e(x, y^-_{j-\frac{1}{2}})}{2} v(x, y^+_{j-\frac{1}{2}})\, dx. \end{aligned} \tag{A.8}$$

We first have $(\Pi_h^\star u - u)_y = 0$ due to the special form of u. Since v_x is a polynomial of degree at most $k-1$ in x, thus from (3.11a), we have

$$\int_{K_{i,j}} \Pi_e v_x \, dxdy = 0, \tag{A.9}$$

and since Π_e is continuous corresponding to the variable y, after applying integration by parts,

we obtain

$$\int_{K_{i,j}} \Pi_e v_y \, dxdy - \int_{I_i} \left(\frac{\Pi_e(x, y^+_{j+\frac{1}{2}}) + \Pi_e(x, y^-_{j+\frac{1}{2}})}{2} v(x, y^-_{j+\frac{1}{2}}) - \frac{\Pi_e(x, y^+_{j-\frac{1}{2}}) + \Pi_e(x, y^-_{j-\frac{1}{2}})}{2} v(x, y^+_{j-\frac{1}{2}}) \right) dx = - \int_{K_{i,j}} (\Pi_e)_y v \, dxdy = 0. \tag{A.10}$$

From Lemma 3.2, we have

$$\begin{aligned} &\Pi_e(x^+_{i+\frac{1}{2}}, y) + \Pi_e(x^-_{i+\frac{1}{2}}, y) \\ =&u(x_{i+\frac{1}{2}}, y) - u(x_{i-\frac{1}{2}}, y) + \Pi^\star_h u(x^+_{i-\frac{1}{2}}) - u(x_{i+\frac{1}{2}}, y) + \Pi^\star_h u(x^-_{i+\frac{1}{2}}, y) - u(x_{i+\frac{1}{2}}, y) \\ =&\Pi^\star_h u(x^+_{i-\frac{1}{2}}) + \Pi^\star_h u(x^-_{i+\frac{1}{2}}, y) - u(x_{i-\frac{1}{2}}, y) - u(x_{i+\frac{1}{2}}, y) \\ =&0. \end{aligned} \tag{A.11}$$

The last equality is from (3.11d). By the same arguments,

$$\Pi_e(x^+_{i-\frac{1}{2}}, y) + \Pi_e(x^-_{i-\frac{1}{2}}, y) = 0. \tag{A.12}$$

From (A.9)-(A.12), we have $b_{i,j}(\Pi_e, v) = 0$. □

Acknowledgments. Research of the first author supported by the China Scholarship Council; Research of the second author supported by NSF grant DMS-1719410; Research of the third author supported by NSFC grant 11871448.

References

[1] J.L. Bona, H. Chen, O. Karakashian and Y. Xing, Conservative, discontinuous Galerkin-methods for the generalized Korteweg-de Vries equation, *Math. Comp.*, **82**:283 (2013), 1401–1432.

[2] Y. Cheng, C.S. Chou, F. Li and Y. Xing, L^2 stable discontinuous Galerkin methods for one-dimensional two-way wave equations, *Math. Comp.*, **86**:303 (2017), 121–155.

[3] C.S. Chou, C.-W. Shu and Y. Xing, Optimal energy conserving local discontinuous Galerkin methods for second-order wave equation in heterogeneous media, *J. Comput. Phys.*, **272** (2014), 88–107.

[4] E.T. Chung and B. Engquist, Optimal discontinuous Galerkin methods for the acoustic wave equation in higher dimensions, *SIAM J. Numer. Anal.*, **47**:5 (2009), 3820–3848.

[5] P.G. Ciarlet, *The Finite Element Method for Elliptic Problems*, North Holland, Amsterdam, New York, 1978.

[6] B. Cockburn and C.-W. Shu, Runge-Kutta discontinuous Galerkin methods for convection-dominated problems, *J. Sci. Comput.*, **16**:3 (2001), 173–261.

[7] J. Du, Y. Yang and E. Chung, Stability analysis and error estimates of local discontinuous Galerkin methods for convection-diffusion equations on overlapping meshes, *BIT Numerical Mathematics*, **59**:4 (2019), 853–876.

[8] D.R. Durran, *Numerical methods for wave equations in geophysical fluid dynamics,* Springer-Verlag, New York, 1999.

[9] G. Fu and C.-W. Shu, Optimal energy-conserving discontinuous Galerkin methods for linear symmetric hyperbolic systems, *J. Comput. Phys.*, **394** (2019), 329–363.

[10] S. Gottlieb, C.-W. Shu and E. Tadmor, Strong stability-preserving high-order time discretization methods. *SIAM Rev.*, **43**:1 (2001), 89–112.

[11] J. Guzmán and B. Rivière, Sub-optimal convergence of non-symmetric discontinuous Galerkin methods for odd polynomial approximations, *J. Sci. Comput.*, **40**:1-3 (2009), 273–280.

[12] N.A. Kampanis, J. Ekaterinaris and V. Dougalis, *Effective Computational Methods for Wave Propagation*, Chapman & Hall/CRC, Boca Raton, 2008.

[13] Y. Liu, C.-W. Shu and M. Zhang, Optimal error estimates of the semidiscrete central discontinuous Galerkin methods for linear hyperbolic equations, *SIAM J. Numer. Anal.*, **56**:1 (2018), 520–541.

[14] Y. Liu, C.-W. Shu and M. Zhang, *Optimal error estimates of the semidiscrete discontinuous Galerkin methods for two dimensional hyperbolic equations on Cartesian meshes using P^k elements*, ESAIM: Mathematical Modelling and Numerical Analysis (ESAIM: M^2AN), **54** (2020), 705-726.

[15] X. Meng, C.-W. Shu and B. Wu, Optimal error estimates for discontinuous Galerkin methods based on upwind-biased fluxes for linear hyperbolic equations. *Math. Comput.*, **85**:299 (2016), 1225–1261.